

2003

Application of Dynamic System Identification to Timber Bridges

S T. Peterson

D I. McLean

Washington State University

David Pollock

George Fox University, dpollock@georgefox.edu

Follow this and additional works at: https://digitalcommons.georgefox.edu/mece_fac



Part of the [Civil Engineering Commons](#), and the [Structural Materials Commons](#)

Recommended Citation

Peterson, S T.; McLean, D I.; and Pollock, David, "Application of Dynamic System Identification to Timber Bridges" (2003). *Faculty Publications - Biomedical, Mechanical, and Civil Engineering*. 40.
https://digitalcommons.georgefox.edu/mece_fac/40

This Article is brought to you for free and open access by the Department of Biomedical, Mechanical, and Civil Engineering at Digital Commons @ George Fox University. It has been accepted for inclusion in Faculty Publications - Biomedical, Mechanical, and Civil Engineering by an authorized administrator of Digital Commons @ George Fox University. For more information, please contact arolfe@georgefox.edu.

Application of Dynamic System Identification to Timber Bridges

S. T. Peterson¹; D. I. McLean²; and D. G. Pollock³

Abstract: A method of global nondestructive evaluation for identifying local damage and decay in timber beams was developed in previous analytical studies and verified experimentally using simply supported beams in the laboratory. The method employs experimental modal analysis and an algorithm that monitors changes in modal strain energy between the mode shapes of a damaged structure with respect to the undamaged structure. A simple three-girder bridge was built and tested in a laboratory to investigate the capability and limitations of the method for detecting damage in a multimember timber structure. The laboratory tests showed that the method can correctly detect and locate a simulated pocket of decay inflicted at the end of a girder as well as detect a notch removed from the midspan of a girder. The tests showed that the method can correctly detect damage simultaneously at two locations within the bridge, but also that large magnitudes of damage at one location can mask smaller magnitudes of damage at another location. When a calibrated baseline model is used to represent the undamaged state of the bridge, the results show that the method of nondestructive evaluation is able to detect each case of inflicted damage, but with some increase in localization error.

CE Database keywords: Bridges, wooden; Vibration tests; Nondestructive tests; Damage.

Introduction

Nondestructive evaluation (NDE) of wood is the science and art of determining the material properties and/or structural capacity of individual members or for an entire timber structure without impairing the member or structure in its usefulness for its intended purpose. A number of methods have been previously developed and implemented in the field of NDE for wood, including visual inspection, stress wave, drill resistance, radiography, ultrasonics, and deflection/vibration analysis (Emerson et al. 1998). Many of these methods are performed on a very localized scale and the evaluation of an entire structure using these methods can be very time consuming and inefficient. Thus, it is desirable to develop a method of nondestructive testing for timber structures that can identify damage or decay from a global perspective. The method investigated in this study is deflection/vibration analysis, specifically experimental modal analysis.

In conjunction with experimental modal analysis, a method for identifying and locating the damage within a structure is needed. In this investigation, a method of damage localization was selected that is based on changes in modal strain energy as an indicator of localized damage or stiffness loss in a structure. In the

literature, this method is often referred to as the damage index method. The method was developed for application to a wide range of structural systems. Previous studies have been published demonstrating the use of the damage index method to localize and estimate the severity of damage within a structure using a limited number of modal parameters for steel plate girders and highway bridges (Bolton et al. 1998; Stubbs et al. 1998). Several analytical studies have been published which verify the performance of this damage localization and severity estimation algorithm (Garcia and Stubbs 1996; Stubbs et al. 1997; Stubbs et al. 2000; Park et al. 2001). A more extensive literature search was presented previously (Peterson et al. 2001a) in support of the selected damage localization algorithm, and an extensive development of the method was given by patented [N. Stubbs, "Apparatus and method for damage detection," U.S. Patent No. 5,327,358 (1994)].

In a previous paper (Peterson et al. 2001a), the method of damage localization was applied to timber beams through analytical evaluations performed on a simply supported timber beam plane stress model. Following the analytical study, experimental impact vibration tests were performed on a timber beam in the laboratory and the damage localization analysis repeated (Peterson et al. 2001b). The experimental tests showed the ability of the damage localization algorithm to successfully detect and locate the inflicted damage. This was done to investigate the capabilities and limitations of using the damage localization algorithm for locating inflicted damage in timber beams.

To further develop the use of the method of global NDE for evaluating a timber structure, a simple bridge model was built in the laboratory to experimentally investigate the capabilities and limitations of the technique in locating damage within a more complex timber system. Damage to the timber bridge was inflicted to represent a pocket of decay at the end of a member as might be typical in an actual timber structure. Other damage cases were designed to investigate the use of the technique for detecting

¹Engineer, BERGER/ABAM Engineers, Inc., Federal Way, WA 98003-2600.

²Professor, Dept. of Civil and Environmental Engineering, Washington State Univ., Pullman, WA 99164-2910.

³Assistant Professor, Dept. of Civil and Environmental Engineering, Washington State Univ., Pullman, WA 99164-2910.

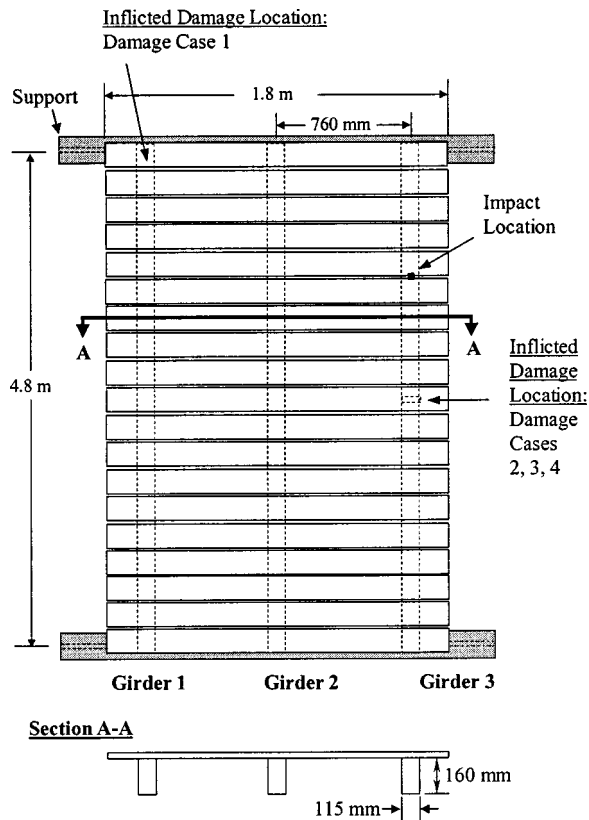


Fig. 1. Plan of laboratory bridge model

and locating small magnitudes of damage and damage at multiple locations within the bridge.

In this paper, the method of damage localization is applied to experimental laboratory tests on a three-girder timber bridge. Based on the results of the experimental testing and damage localization analyses, the effectiveness of using the method of global NDE for identifying damage or decay in timber structures is demonstrated. The laboratory tests were conducted in an effort to investigate the applicability of the method of NDE to performing a global evaluation of a timber structure to identify and locate possible areas of damage or decay. The areas identified within the timber structure by the global evaluation would then be investigated further using a more localized form of NDE (e.g., ultrasonics) to confirm the damage and better assess the magnitude or severity of the damage or decay. Depending on the location and magnitude of the damage or decay, a decision would then be made to repair or replace the damaged member to maintain the integrity and usefulness of the structure.

Three-Girder Laboratory Bridge

A three-girder laboratory bridge model was built at Washington State University to apply the technique of dynamic system identification to a timber system. The bridge, shown in Figs. 1 and 2, consisted of three girders measuring 115 mm (4.5 in.) \times 160 mm (6.25 in.) in cross section with a span of 4.8 m (15 ft.–10 in.). The decking boards were 25 mm (1 in.) \times 150 mm (6 in.) in cross section and 1.8 m (6 ft.) long. The longitudinal modulus of elasticity (MOE) values E_x as determined by stress wave time for each of the three girders and the deck boards are shown in Table 1. The ends of the bridge girders were supported on steel I beams

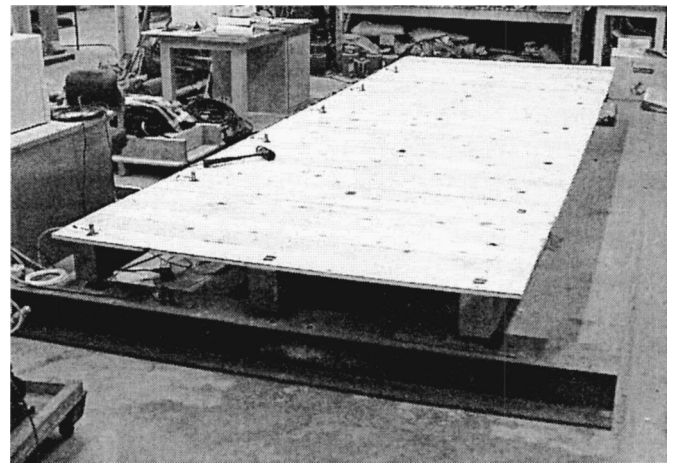


Fig. 2. Laboratory bridge model

as shown in Fig. 2. Steel pin supports were fabricated and inserted between the bridge girders and the supporting steel beam directly over the web of the I beam.

Experimental modal tests were performed on the undamaged laboratory bridge to obtain the modal parameters needed—natural frequencies of vibration and corresponding mode shapes. Accelerometers were placed on the top of the bridge deck located over the supports and at 1/6 points along the span as shown in Fig. 2. Three different configurations of the accelerometers were used to obtain the modal parameters of the bridge. For the first configuration, the accelerometers were set up as described, directly over the center of Girder 1. For Configurations 2 and 3, the accelerometers were similarly located directly over the center of Girder 2 and Girder 3, respectively. For each configuration of accelerometer setup, the bridge was excited into its modes of vibration by impacting the bridge directly over the center of Girder 3 at the $\frac{3}{4}$ point along the span. This impact location along Girder 3 was selected so that both flexural and torsional modes of vibration in the bridge could be excited simultaneously, and the $\frac{3}{4}$ point was selected so that the first and second flexural modes could be excited in the simply supported timber bridge. Data acquisition was used to record data from each accelerometer and from the instrumented impact hammer at 1,000 Hz sampling rate for 4,096 points of data. To improve the experimentally obtained mode shape coordinates, the impact tests were repeated ten times for each accelerometer configuration in order to average out some of the noise present in the experimental measurements. A statistical analysis of the experimental data obtained from tests 1–10 showed that the coefficient of variation between mode shape coordinate values was below 9%. From the experimental tests, five modes of vibration were obtained. The mode shapes are shown in Fig. 3, and the natural frequencies of vibration for the pristine or undamaged structure are given in Table 3. It should be noted that

Table 1. Longitudinal Modulus of Elasticity of Bridge Girders and Decking

	E_x GPa (psi)
Girder 1	13.93 (2.02 $\times 10^6$)
Girder 2	11.78 (1.71 $\times 10^6$)
Girder 3	13.27 (1.92 $\times 10^6$)
Decking	9.17 (1.33 $\times 10^6$)

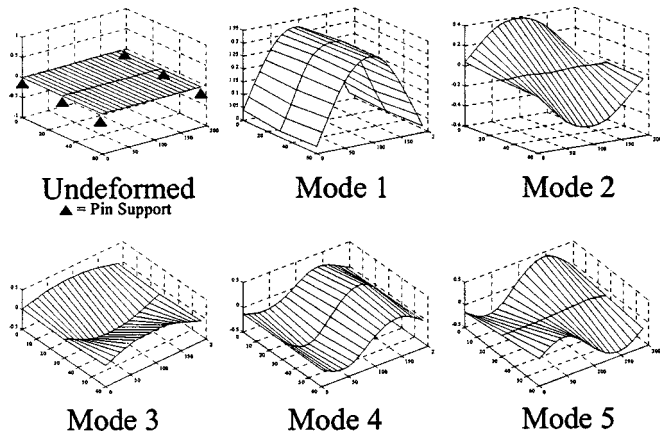


Fig. 3. Experimentally obtained mode shapes

transverse bending modes were ignored because these modes were not specifically excited and did not show up in the frequency response function data.

Inflicted Damage

Once the modal parameters for the undamaged bridge model were determined, damage was inflicted on the bridge. Since it was of interest to test the ability of the technique to locate damage and decay typically found in timber structures, Damage Case 1 consisted of a pocket removed from the end of Girder 1 to simulate a pocket of decay. Inspection of actual decay at the ends of timber beams shows a region or pocket of decayed wood that crumbles easily and does not contribute at all to the stiffness at the end of

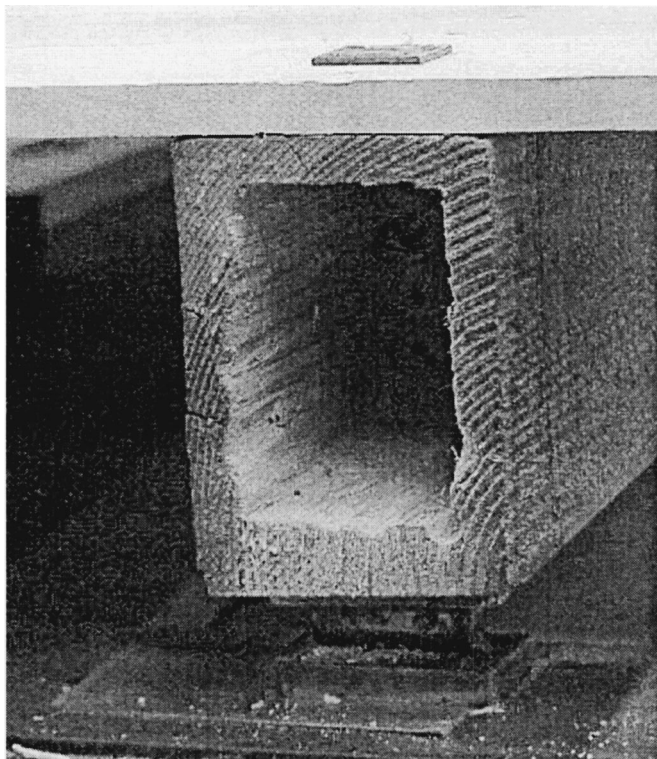


Fig. 4. Simulated pocket of decay—Damage Case 1

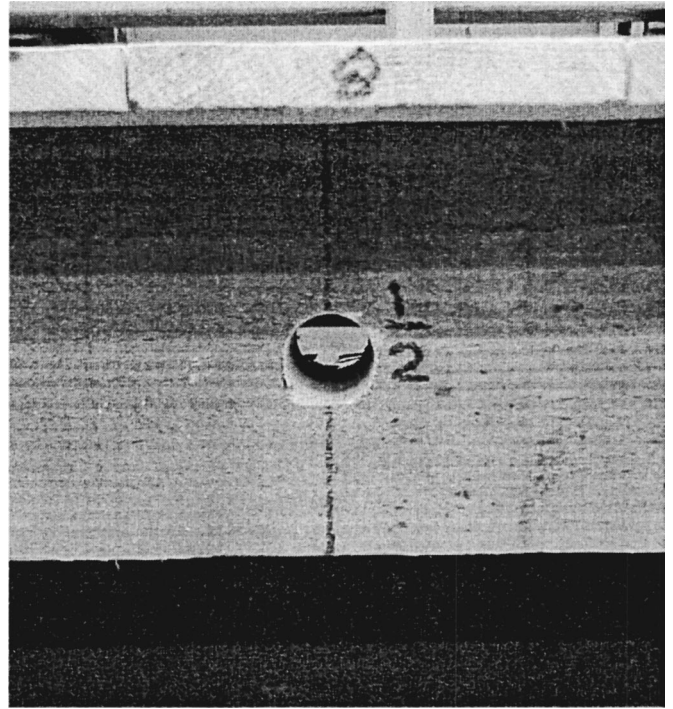


Fig. 5. Inflicted Damage Case 2

the beam. Located around the region of decay is a “shell” of semisound wood that acts alone to transfer load to the supporting elements or foundation on which the beam is supported. Thus, to simulate decay at the end of Girder 1, a pocket of sound wood was removed as shown in Fig. 4. The removed pocket measured approximately 85 mm (3.38 in.) \times 125 mm (4.88 in.) \times 235 mm (9.25 in.) deep. This left a shell of sound wood approximately 20-mm (0.75 in.) thick around the perimeter of the cross section at the end of Girder 1. It should be noted that the damage inflicted for Damage Case 1 was present through all of the subsequent tests.

Damage Case 2 consisted of a 32-cm (1.25 in.) diameter hole drilled through the neutral axis of Girder 3, located at midspan (Fig. 5). For the tests conducted on the bridge, the sensitivity of the technique in correctly detecting smaller magnitudes of damage was of interest. Damage Case 2 corresponds to a 0.8% reduction in the bending moment of inertia of the girder cross section. A hole through the neutral axis was first inflicted, and subsequent tests considered cases in which this hole was extended as a notch that stretched progressively toward the bottom face of Girder 3. The dimensions of the notch used to simulate damage for the various cases are given in Table 2. Damage Case 3 is shown in Fig. 6. For Damage Case 4, the notch is extended through the tension face of Girder 3.

The modal impact tests as described previously for the modal tests conducted on the undamaged bridge were repeated for each of the damage cases considered. The modal parameters were ob-

Table 2. Dimensions of Inflicted Damage

Damage Case	Notch width cm (in.)	Notch depth cm (in.)
2	3.18 (1.25)	3.18 (1.25)
3	3.18 (1.25)	6.35 (2.5)
4	3.18 (1.25)	8.89 (3.5)

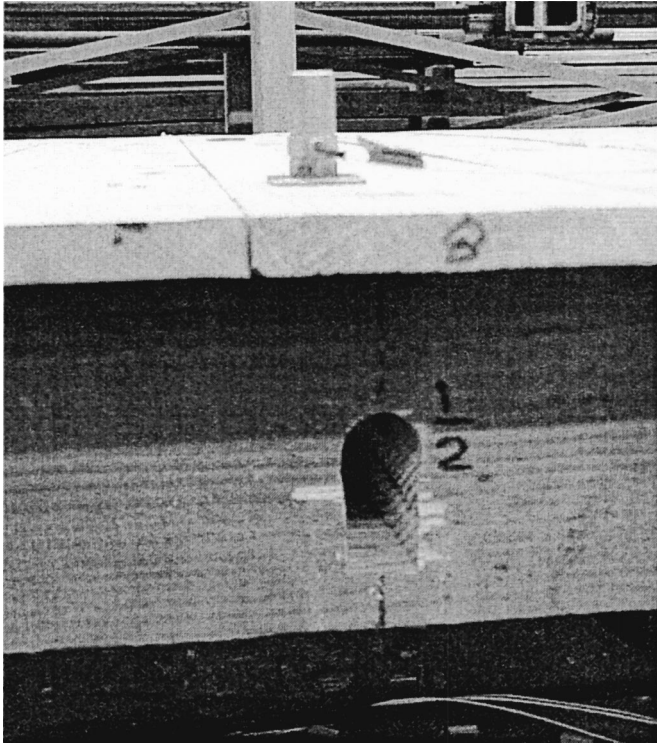


Fig. 6. Inflicted Damage Case 3

tained and the experimental mode shapes were used with the damage localization algorithm to try to locate the inflicted damage. The natural frequencies of vibration identified for each of the Damage Cases are shown in Table 3.

Damage Localization Algorithm

To localize the inflicted damage within the bridge model, a method of damage localization developed previously (Stubbs et al. 1995) was used. The damage localization algorithm was derived such that differences in modal strain energy between the undamaged structure and the damaged structure provide a basis for identification of localized damage. Shannon's sampling theory (Park and Stubbs 1995; Stubbs and Park 1996) was used to interpolate the experimental mode shapes and divide the structure into j elements. The algorithm used to calculate the damage indicator for the j th element and the i mode, β_{ij} , is given below.

Table 3. Natural Frequencies of Vibration

Damage	Mode 1 f_1 (Hz)	Mode 2 f_2 (Hz)	Mode 3 f_3 (Hz)	Mode 4 f_4 (Hz)	Mode 5 f_5 (Hz)
Undamaged	12.207	14.160	22.949	42.969	48.096
1 ^a	11.963	13.916	22.705	41.504	46.387
2 ^b	11.963	13.916	22.705	41.504	46.143
3 ^c	11.474	13.428	22.949	41.748	45.410
4 ^d	10.253	12.939	22.461	41.259	45.654

^aSimulated pocket of decay at end of Girder 1.

^b32-mm diameter hole through NA of Girder 3 at midspan.

^cHole of Case 2 extended toward tension face as a notch.

^dNotch extended through tension face of Girder 3.

$$\beta_{ij} = \frac{1 + F_{ij}^*}{1 + F_{ij}} = \frac{\left[\int_j \{\phi_i''^*(x)\}^2 dx + \int_0^L \{\phi_i''^*(x)\}^2 dx \right] \int_0^L \{\phi_i''(x)\}^2 dx}{\left[\int_j \{\phi_i''(x)\}^2 dx + \int_0^L \{\phi_i''(x)\}^2 dx \right] \int_0^L \{\phi_i''^*(x)\}^2 dx} \quad (1)$$

The derivation of Eq. (1) is discussed in Stubbs et al. (1995) or Peterson et al. (2001a). It should be noted that the terms $\phi_i(x)$ in Eq. (1) are vectors of mode shape coordinates for a single beam or girder, but denote a matrix describing the mode shape corresponding to Mode i for a bridge or structure. Previously, each of the mode shape vectors were divided by its Euclidean norm to normalize the mode shape. Here again, each mode shape coordinate in the mode shape matrix was divided by the Euclidean norm of the matrix to obtain a normalized mode shape matrix. To simplify the damage localization analysis, the mode shape matrix was split into three mode shape vectors, one for each of the girders used for the bridge. The damage localization algorithm was then used to compare the normalized mode shape vector for each girder from each of the damage cases versus the corresponding normalized undamaged mode shape vector. To account for all of the modes available, NM, the damage indicator value for a single element j is given as

$$\beta_j = \frac{\sum_{i=1}^{NM} \text{NUM}_{ij}}{\sum_{i=1}^{NM} \text{DENOM}_{ij}} \quad (2)$$

where NUM_{ij} =numerator of β_{ij} in (1) and DENOM_{ij} =denominator of β_{ij} in Eq. (1).

Finally, the damage indicator values for each element j are transformed into the standard normal space and hypothesis testing is used to classify the elements into one of two classes: (1) the element j is undamaged or (2) the element j is damaged. Damage indicator values are transformed into the standard normal space using the following equation:

$$Z_j = \frac{\beta_j - \mu_{\beta_j}}{\sigma_{\beta_j}} \quad (3)$$

where μ_{β_j} =mean of β_j values for all j elements and σ_{β_j} =standard deviation of β_j for all j elements. A threshold value is judgmentally selected and used to determine which of the j elements are possibly damaged (e.g., $Z_j > 2$ indicates damage at Member j within a 95% confidence interval). The threshold level is left to the user to define based on what level of confidence is required for localization of damage within the structure. If the global method of damage localization is used in conjunction with other more localized methods of detection, a lower threshold may be permissible. This would likely result in a higher number of indications of damage (including false positives) which could then be investigated further using a more localized method of detection.

Damage Localization: Experimental Parameters

To perform the damage localization analysis, the damaged mode shape vectors were compared to the corresponding undamaged mode shape vectors using the damage localization algorithm given previously. The analysis was made on a girder by girder basis to investigate the ability of the algorithm to localize the inflicted damage present within the bridge model. For the analy-

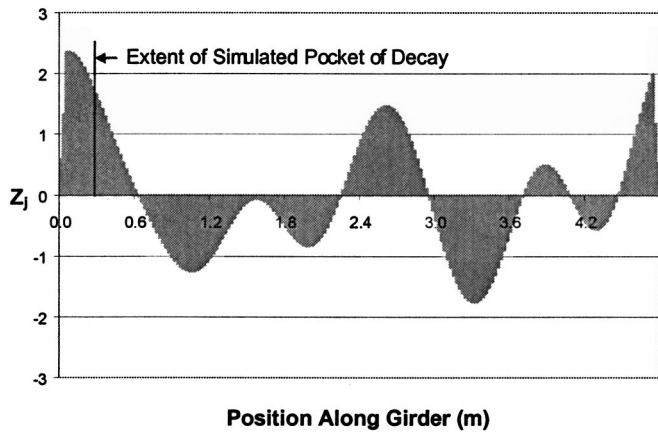


Fig. 7. Damage indicator values for Damage Case 1, Girder 1, Modes 4 and 5 considered

sis, the threshold Z_j value was generally set at $Z_j > 2$ indicative of damage at Element j within a 95% confidence interval. Wherever more than one mode of vibration was used to localize the inflicted damage, the modes were combined as given in Eq. (2).

From the results of the analysis for Damage Case 1, it was concluded that the algorithm was able to correctly detect and locate the simulated pocket of decay at the end of Girder 1. The damage indicator values ranged between 2.0 and 2.4 over the extent of the simulated pocket of decay. Fig. 7 is a plot of damage indicator values for Girder 1 corresponding to Damage Case 1. Modes 4 and 5 were the most sensitive to damage present at the end of a girder. Consequently, these were the only mode shapes used to localize the inflicted damage for Case 1. In considering Modes 4 and 5, the damage localization algorithm showed only one false positive indication of damage over the other areas of the bridge, located near the 1/3 point of Girder 2.

For Damage Case 2, the analysis showed some indication of damage near the midspan of Girder 3. However, the algorithm indicated that the damage was located approximately 230 mm (9 in.) away from the correct location at the midspan of Girder 3. Due to the location of the inflicted damage for Cases 2–4, Modes 1, 2, and 3 were the most sensitive to the effects of the damage. Thus, Modes 1, 2, and 3 were used to attempt to detect and locate the inflicted damage. Damage indicator values for Girder 3 are

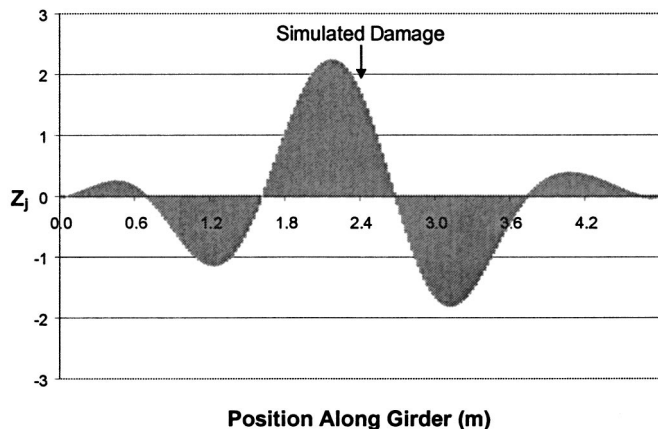


Fig. 8. Damage indicator values for Damage Case 2, Girder 3, Modes 1, 2, and 3 considered

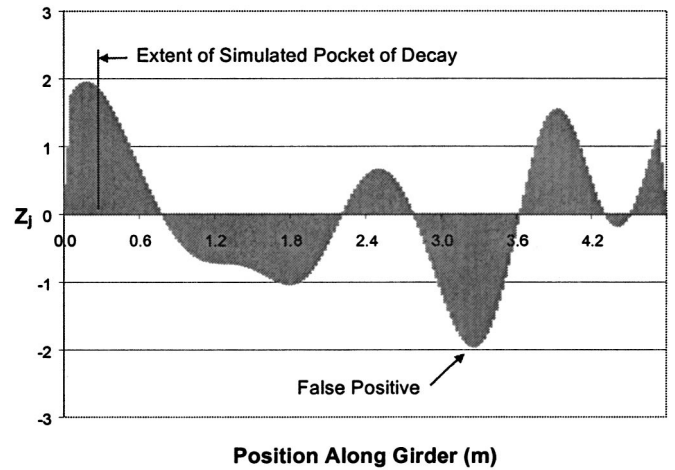


Fig. 9. Damage indicator values for Damage Case 2, Girder 1, Modes 4 and 5 considered

shown in Fig. 8. Considering Modes 1, 2, and 3, the damage localization algorithm also showed one false positive indication of damage at the midspan of Girder 1.

In addition to the inflicted damage at the midspan of Girder 3, the damage localization algorithm was also able to correctly detect the simulated pocket of decay present at the end of Girder 1 if the threshold is set at $Z_j > 1.9$ (94% confidence interval). Again, Modes 4 and 5 were used to locate the simulated pocket of decay. In the presence of the inflicted damage at Girder 3, the damage localization algorithm shows one false positive indication of damage located at 3.3 m in Girder 1. The damage localization algorithm also showed two additional false positive indications of damage within the bridge, located along Girders 2 and 3. Fig. 9 shows the ability to localize the simulated pocket of decay in Girder 1 with the additional damage to Girder 3 also present.

For the analysis of Damage Case 3, the damage localization algorithm demonstrated a more precise localization of the increased severity of inflicted damage at the midspan of Girder 3. The plot of damage indicator values in Fig. 10 shows the damage located approximately 110 mm (4.3 in.) away from the correct location of the inflicted damage. However, the analysis also showed two additional false positive indications of damage, lo-

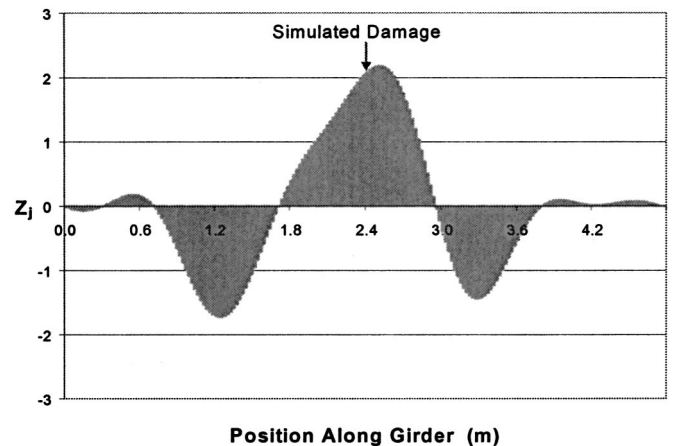


Fig. 10. Damage indicator values for Damage Case 3, Girder 3, Modes 1, 2, and 3 considered

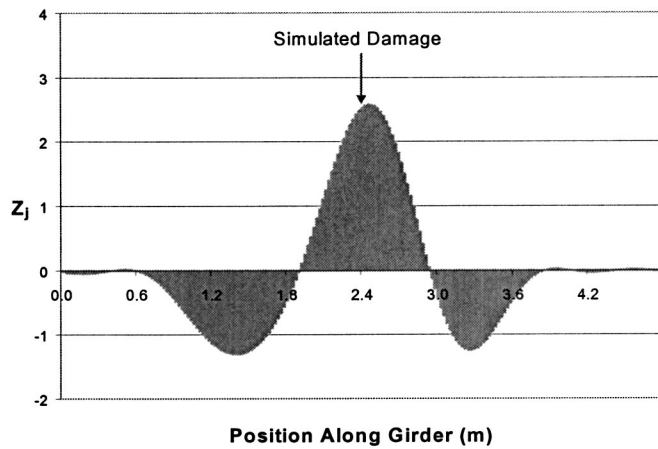


Fig. 11. Damage indicator values for Damage Case 4, Girder 3, Modes 1, 2, and 3 considered

cated along Girders 1 and 2. With the increased severity of damage located at the midspan of Girder 3, the algorithm was no longer able to correctly detect and locate the simulated pocket of decay at the end of Girder 1.

Finally, for Damage Case 4, the damage localization algorithm was able to correctly detect and locate the inflicted damage very near the exact location at the midspan of Girder 3. The algorithm was able to locate the damage within 60 mm (2.4 in.) from the correct location of the inflicted damage. The analysis showed only one additional false positive indication of damage along Girder 1. As with Damage Case 3, the simulated pocket of decay at the end of Girder 1 could no longer be detected. Fig. 11 shows the damage indicator values for Damage Case 4. Table 4 shows a summary of the performance of the damage localization algorithm in identifying and locating the damage inflicted on the bridge when experimental undamaged modal parameters are used.

Calibrated Baseline Model

Since the modal parameters for an as-built or pristine timber structure in the field will be unknown, the undamaged structure must be modeled using a computer analysis to approximate the baseline modal parameters. To do this for the laboratory bridge, a finite-element model consisting of three-dimensional (3D) beam elements was developed. A stress wave timer was used in the laboratory to obtain initial values for the stiffness properties of the structural members used to build the bridge. The model was developed using the initial stiffness values and was calibrated according to the calibration process described by Stubbs and Osegueda (1990a,b) and Stubbs and Kim (1996) using the experimentally measured natural frequencies of vibration.

Table 4. Performance of Damage Localization Analysis: Experimental Parameters

Damage	Girder 3 damage identified	Girder 1 damage identified	Damage indicator magnitude	Localization error cm (in.)	False positives
1	—	Yes	2.0–2.4	0	1
2	Yes	Yes	2.2	23 (9)	1
3	Yes	No	2.2	11 (4.3)	2
4	Yes	No	2.6	6 (2.4)	1

Table 5. Natural Frequencies of Vibration

Mode	Experimental undamaged f_i (Hz)	Calibrated baseline model f_i (Hz)	Percent difference
1	12.207	12.262	-0.45
2	14.160	14.255	-0.67
3	22.949	23.378	-1.87
4	42.969	44.996	-4.72
5	48.096	51.239	-6.54

The material properties modified to calibrate the finite-element model included the support stiffness, the longitudinal modulus of elasticity (MOE) of each of the three girders (separately), and the longitudinal MOE of the decking members (uniformly). Though the stiffness of the supports in the laboratory were not experimentally quantified, the tests showed small modal displacements at the ends of each girder. The support stiffnesses of the finite-element model were adjusted such that the output mode shapes had similar end displacements as were obtained from the experimental mode shapes. The remaining calibration of the baseline model was made by adjusting the stiffness of the girders and the decking until the natural frequencies of the finite-element model closely matched those measured experimentally. The natural frequencies of the calibrated model are given in Table 5. The stiffness properties for each of the structural members initially measured using stress wave times as well as the stiffness properties of the calibrated baseline model are given in Table 6 and show that the calibration process yielded a reasonable model of the laboratory bridge. The large difference between measured and calibrated E_x values for the decking members may also include assumptions involving the connection of the deck members to the girders. Full composite action was assumed for the computer model while the laboratory model is likely less than fully composite. Thus, the large difference in E_x values for the decking members is not considered an indication of an unreasonable baseline model of the laboratory bridge.

A frequency analysis was performed on the calibrated finite-element model to obtain the modal parameters needed. The mode shapes for the first five modes were output and interpolated using Shannon's sampling theory used in place of the experimentally measured mode shapes for the undamaged state of the bridge.

Use of Calibrated Baseline Model For Damage Localization

Using the mode shapes from the calibrated baseline model in place of the experimental mode shapes for the undamaged state of the bridge, the analyses were repeated to try to localize the inflicted damage for the situation where the undamaged or baseline modal parameters were unknown. For Damage Case 1, Modes 4

Table 6. Material Property Values

	Experimental (stress wave) GPa (psi)	Calibrated baseline model GPa (psi)
E_x - Girder 1	13.94 (2.02 × 10 ⁶)	15.65 (2.27 × 10 ⁶)
E_x - Girder 2	11.78 (1.71 × 10 ⁶)	11.05 (1.60 × 10 ⁶)
E_x - Girder 3	13.27 (1.92 × 10 ⁶)	13.30 (1.93 × 10 ⁶)
E_x - Decking	9.17 (1.33 × 10 ⁶)	5.47 (0.79 × 10 ⁶)

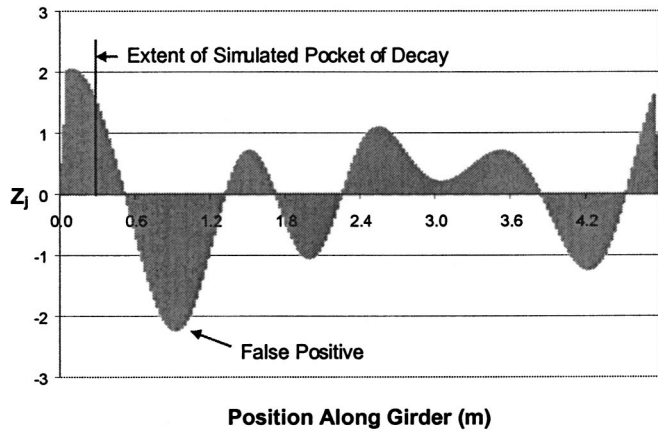


Fig. 12. Damage indicator values for Damage Case 1, calibrated baseline model Girder 1, Modes 4 and 5 considered

and 5 are considered and the simulated pocket of decay was correctly located at the end of Girder 1. In using the mode shapes from the calibrated baseline model to approximate the undamaged modal parameters, the algorithm identifies the simulated pocket of decay from the end of Girder 1 to approximately 180-mm (7 in.) deep. Since the removed pocket extended 235 mm (9.25 in.) into the end of Girder 1, the error in damage localization is 50 mm (2 in.). In addition, one false positive indication of damage along Girder 1 was identified. Considering Modes 4 and 5 for Girders 2 and 3, only one false positive indication of damage is shown along Girder 2. The damage indicator values for Damage Case 1 are shown in Fig. 12.

In considering Damage Case 2, the damage localization algorithm gives some indication of the 32-mm diameter (1.25 in.) hole drilled through the neutral axis of Girder 3, but the damage is identified 43 mm (1.67 in.) away from the true location of the inflicted damage. Modes 1, 2, and 3 were used to identify and locate the inflicted damage at the midspan of Girder 3. For the analysis of the inflicted damage at the midspan of Girder 3, the algorithm also showed two false positive indications of damage located along Girders 1 and 2. Fig. 13 shows the damage indicator values for Damage Case 2 with the calibrated baseline model used to approximate the baseline modal parameters.

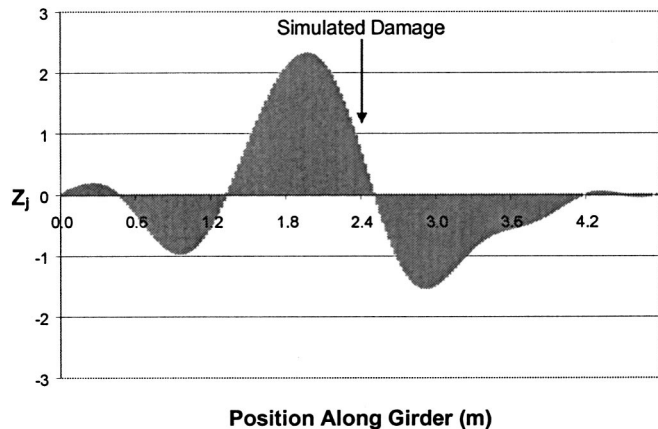


Fig. 13. Damage indicator values for Damage Case 2, calibrated baseline model Girder 3, Modes 1, 2, and 3 considered

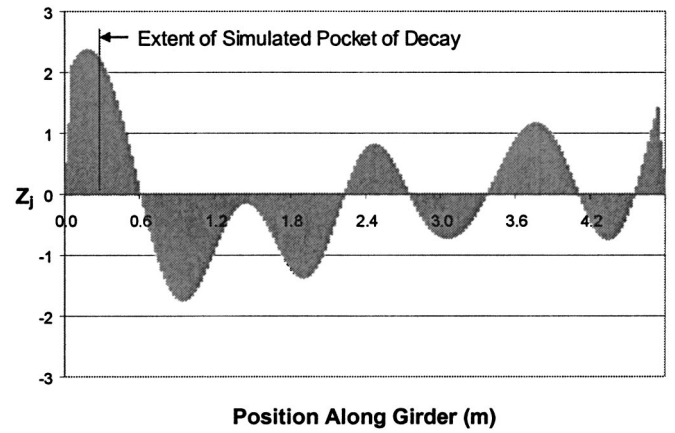


Fig. 14. Damage indicator values for Damage Case 2, calibrated baseline model, Girder 1, Modes 4 and 5 considered

When the inflicted damage corresponding to Damage Case 2 is present, the simulated pocket of decay at the end of Girder 1 is also correctly identified using Modes 4 and 5. For the analysis of Damage Case 2, the algorithm performed better in correctly detecting the simulated pocket of decay than for the analysis of Damage Case 1 (Fig. 14). However, two false positive indications of damage within the bridge are also identified by the analysis.

Using Modes 1, 2, and 3 for the analysis of Damage Case 3, the damage localization algorithm gave an indication of the inflicted damage at the midspan of Girder 3 with an increased precision in the damage localization. Fig. 15 shows that the algorithm identified the damage approximately 330 mm (12.9 in.) away from the true location of the inflicted damage. For Damage Case 3, only one false positive indication of damage is identified along Girder 2. As previously observed, the simulated pocket of decay at the end of Girder 1 could not be correctly localized with the increased magnitude of inflicted damage for Case 3 present at the midspan of Girder 3.

For Damage Case 4, the analysis showed that the damage localization algorithm identified the inflicted damage within 110 mm (4.3 in.) of the correct location. Fig. 16 shows the damage indicator values along Girder 3 for Damage Case 4 considering Modes 1, 2, and 3. Upon reviewing the results for Girders 1 and 2, only one false positive indication of damage is identified along

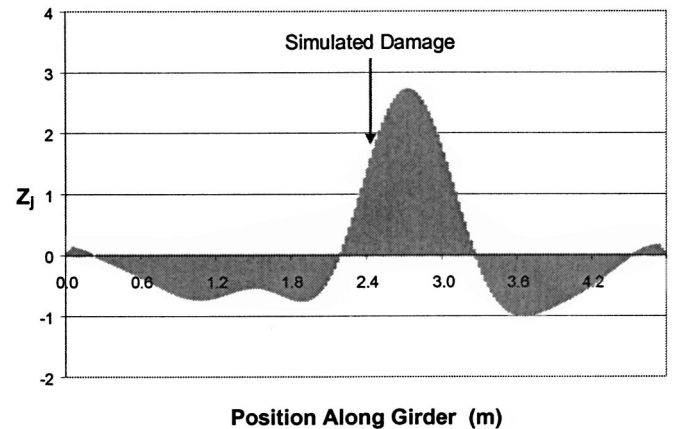


Fig. 15. Damage indicator values for Damage Case 3, calibrated baseline model, Girder 3, Modes 1, 2, and 3 considered

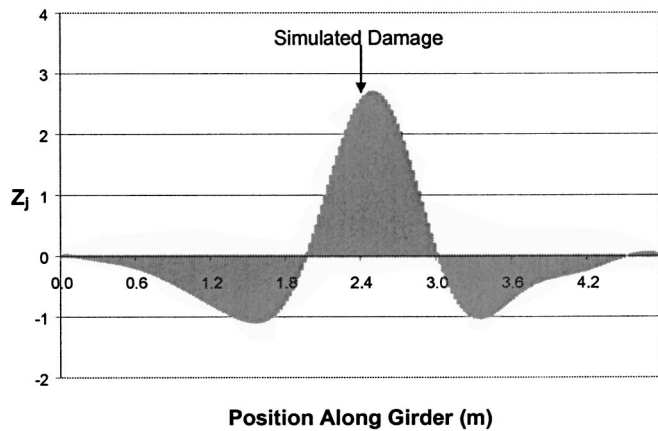


Fig. 16. Damage indicator values for Damage Case 4, calibrated baseline model, Girder 3, Modes 1, 2, and 3 considered

Girder 2. Table 7 shows a summary of the performance of the damage localization algorithm in identifying and locating the damage inflicted on the bridge when the calibrated baseline model is used to approximate the undamaged modal parameters.

Conclusions

The impact vibration tests conducted in the laboratory and subsequent damage localization analysis showed that the simulated pocket of decay inflicted in the end of Girder 1 can be correctly identified for simulated decay extending 235 mm (9.25 in.) into the girder. In addition, inflicted damage equivalent to a 0.8% reduction in the bending moment of inertia of Girder 3 can also be correctly identified at the midspan of the girder. For Damage Cases 2–4, as the magnitude of the inflicted damage at the midspan of Girder 3 was increased, the magnitude of the damage indicator values also increased. This is a similar trend to that found for simply supported timber beams (Peterson et al. 2001b). Using the standard normal damage indicator values and hypothesis testing discussed previously, this indicates that the inflicted damage can be detected more confidently as the severity of damage increases. In addition to the increased confidence of damage detection, the analysis also shows that the algorithm used has more precision in correctly locating the inflicted damage as the severity increases.

For the analysis following Damage Case 2, the analysis was able to correctly detect and locate the simulated pocket of decay at the end of Girder 1 as well as the damage at the midspan of Girder 3. However, the ability to detect the simulated pocket of decay is lost as the severity of damage at the midspan of Girder 3 is increased to Damage Case 3. From the experimental Damage

Table 7. Performance of Damage Localization Analysis: Calibrated Baseline Parameters

Damage	Girder 3 damage identified	Girder 1 damage identified	Damage indicator magnitude	Error cm (in.)	False positives
1	—	Yes	1.7–2.0	5.1 (2)	2
2	Yes	Yes	2.3	42.4 (16.7)	2
3	Yes	No	2.7	32.8 (12.9)	1
4	Yes	No	2.7	10.9 (4.3)	1

Cases considered, it is concluded that the presence of the increased magnitude of localized damage at the midspan of Girder 3 may have had a dominating effect on the lower modes of vibration such that the simulated pocket of decay at the end of Girder 1 could no longer be detected. In the interest of applying this method of localized damage detection to actual timber structures, it is noted that the presence of larger magnitudes of damage in one area of the structure may prevent the detection of smaller magnitudes of damage at other locations within the structure.

Since the undamaged modal parameters will not be available for an actual timber structure, a finite-element model was constructed and calibrated to represent the undamaged state of the bridge. When the undamaged modal parameters of the bridge are approximated using the calibrated baseline model, the analysis again demonstrated the ability to detect each of the damage cases. However, using approximate modal parameters for the undamaged state of the bridge in the analysis resulted in greater localization error. Similar trends are noted in confidence of damage detection and error in localization for the analysis using the calibrated baseline model as for the analysis using the experimental undamaged modal parameters.

One or two false positive indications of damage were shown for each of the analyses conducted. As discussed by Stubbs and Garcia (1996a), the damage localization algorithm is prone to false positive indications of damage when, simultaneously, the element size becomes small and the element is located at the node point of a mode shape. It was noted that, for the majority of the false positive indications of damage encountered in the analyses, the false positive was near a possible node point for either Mode 2 or Mode 5 within Girder 2. While the tendency of the algorithm to make false positive indications of damage is due to a mathematical instability, the algorithm actually performed very well in indicating only one or two false positives over the entire bridge. Furthermore, the identification of several false positive indications of damage in an actual field investigation of a timber structure would mean that a small number of additional areas of the bridge would need to be investigated further using more localized forms of NDE, such as ultrasonics. This is not considered prohibitive in applying the technique to the nondestructive evaluation of a timber structure.

Based on the performance of the method of global NDE with the inflicted damage cases in the laboratory bridge, it is concluded that the method of global evaluation can be used with other more localized methods to perform a field evaluation of an actual timber structure. When used in conjunction with other more localized forms of NDE, the tendency of the algorithm to make false positive identifications of damage poses only a small problem. A more significant obstacle in implementing the use of the method of NDE is that large magnitudes of damage or decay at one location within the structure may mask or hide smaller magnitudes of damage or decay at other locations. From the analyses presented here, as well as past experience in applying the method of NDE to timber beams (Peterson et al. 2001a,b), it is recommended that the analysis consider each of the available modes independently as well as combined to make the best overall evaluation of the timber structure.

Acknowledgments

Funding for this project was provided by the U.S. Federal Highway Administration and the USDA Forest Service Forest Products Laboratory.

Notation

The following symbols are used in this paper:

- E_x = longitudinal modulus of elasticity;
 F_{ij}, F_{ij}^* = fraction of modal strain energy concentrated in Element j for Mode i ;
 f_i = natural frequency of vibration for Mode i (Hz);
 i = index of natural frequency of vibration, mode;
 j = index of element within bridge/structure;
 Z_j = standard normal damage indicator value for element j ;
 β_{ij} = damage indicator value for Mode i , Element j ;
 μ_{β_j} = mean of β_j values for all j elements;
 σ_{β_j} = standard deviation of β_j values for all j elements;
and
 ϕ_{ij} = mode shape coordinate for Mode i , Element j .

References

- Bolton, R., Stubbs, N., Park, S., and Choi, H. (1998). *Analysis of lavic road overcrossing field data*, Texas A&M University Press, Engineering Technology, Lubbock, Tex.
- Emerson, R. N., Pollock, D. G., Kainz, J. A., Fridley, K. J., McLean, D. I., and Ross, R. J. (1998). "Nondestructive evaluation techniques for timber bridges." *Proc., 1998 World Conf. on Timber Engineering (WCTE)*, Lausanne, Switzerland, 670–677.
- Garcia, G., and Stubbs, N. (1996). "Application of pattern recognition to damage localization." *Microcomput. Civ. Eng.*, 11, 395–409.
- Park, S., and Stubbs, N. (1995). "Reconstruction of mode shapes using Shannon's sampling theorem and its application to nondestructive damage localization algorithm." *Proc. SPIE*, 2446, 280–292.
- Park, S., Stubbs, N., Bolton, R., Choi, S., and Sikorsky, C. (2001). "Field verification of the damage index method in a concrete box-girder bridge via visual inspection." *Int. J. Comput. Aided Civil and Infra-Structure Eng.*, 16, 58–70.
- Peterson, S. T., McLean, D. I., Symans, M. D., Pollock, D. G., Cofer, W. F., Emerson, R. N., and Fridley, K. J. (2001a). "Application of dynamic system identification to timber beams: I." *J. Struct. Eng.*, 127(4), 418–425.
- Peterson, S. T., McLean, D. I., Symans, M. D., Pollock, D. G., Cofer, W. F., Emerson, R. N., and Fridley, K. J. (2001b). "Application of dynamic system identification to timber beams: II." *J. Struct. Eng.*, 127(4), 426–432.
- Stubbs, N., and Garcia, G. (1996). "Application of pattern recognition to damage localization." *Microcomput. Civ. Eng.*, 11, 411–419.
- Stubbs, N., and Kim, J. T. (1996). "Damage localization in structures without baseline modal parameters." *AIAA J.*, 34(8), 1644–1649.
- Stubbs, N., Kim, J. T., and Farrar, C. R. (1995). "Field verification of a nondestructive damage localization and severity estimation algorithm." *Proc., 13th Int. Modal Analysis Conf.*, Nashville, Tenn., 210–218.
- Stubbs, N., and Osegueda, R. (1990a). "Global nondestructive damage evaluation in solids." *Int. J. Anal. Exp. Modal Anal.*, 5(2), 67–79.
- Stubbs, N., and Osegueda, R. (1990b). "Global damage detection in solids—Experimental verification." *Int. J. Anal. Exp. Modal Anal.*, 5(2), 81–97.
- Stubbs, N., and Park, S. (1996). "Optimal sensor placement for mode shapes via Shannon's sampling theorem." *Microcomput. Civ. Eng.*, 11, 411–419.
- Stubbs, N., Park, S., and Sikorski, C. (1997). "A general methodology to non-destructively evaluate bridge structural safety." *Technical Rep. No. NDD 04-97-04 Submitted to State of California, Dept. of Transportation, Sacramento, Calif.*, Texas Engineering Experimental Station, Texas A&M Univ., College Station, Tex.
- Stubbs, N., Park, S., Sikorski, C., and Choi, S. (2000). "A global non-destructive damage assessment methodology for civil engineering structures." *Int. J. Syst. Sci.*, 31(11), 1361–1373.
- Stubbs, N., Sikorsky, C., Park, S., Choi, S., and Bolton, R. (1998). "A methodology to nondestructively evaluate the structural properties of bridges." *Proc., 5th CALTRANS Seismic Research Workshop*, California Dept. of Transportation Service Center, Sacramento, Calif.